Icarus **143**, 147–154 (2000)
doi:10.1006/icar.1999.6235, available online at http://www.idealibrary.com on IDEAL®

ISOPHOT Observations of Dust Disks around Main Sequence (Vega-Like) Stars

H. J. Walker

CLRC Rutherford Appleton Laboratory, Chilton, Didcot, Oxfordshire OX11 0QX, United Kingdom
E-mail: h.j.walker@rl.ac.uk

and

I. Heinrichsen

IPAC, MS 100-22,California Institute of Technology, Pasadena, California 91125

Received September 15, 1998; revised June 24, 1999

The photometer (ISOPHOT) on the Infrared Space Observatory (ISO) has proved to be invaluable for investigating the dust around main sequence stars (both prototypes and candidate Vega-like stars). The long wavelength camera (at 60 and 90 μm) has been used to map the area around the stars to establish whether the dust disk is extended. Low-resolution spectra between 5.8 and 11.6 μm show whether the dust is composed of silicate grains, and whether molecular features are present. The four prototype Vega-like stars (Vega, β Pic, Fomalhaut, ϵ Eri) are studied, as well as eight other stars, which are main sequence stars with cool dust associated with them. We find that the spectra of β Pic, 49 Cet, HD98800, and HD135344 show excess emission from the cool dust around the star, HD144432 and HD139614 show silicate dust emission, HD169142 and HD34700 show emission features from carbon-rich molecules (possibly PAHs, polycyclic aromatic hydrocarbon molecules), and HD142666 shows emission features from both carbon-rich molecules and silicate dust. Up to 11.6 μm, the emission from Vega, Fomalhaut, and ϵ Eri is dominated by the stellar photosphere. At 60 and 90 μm, the extended dust emission is mapped, and the disk resolved in eight cases. The dust mass in the disks is found to range from around 10^{-9} to 10^{-4} $M_{\odot}$. Since several of the stars are younger than the Sun, and the disks have sufficient material of the type found in the Solar System, these disks could be in the early stages of planet formation. © 2000 Academic Press

Key Words: **Vega-like stars; infrared observations; extrasolar planets; planetary formation.**

I. INTRODUCTION

Four normal main sequence stars (Vega (α Lyr), β Pic, Fomalhaut (α PsA), and ϵ Eri), were found by the IRAS satellite to have dust disks around them (Aumann *et al.* 1984, Gillett 1986). These became the prototype Vega-like stars. The dust disks were cool (around 100 K) and tenuous, with masses of order Moon mass rather than Jupiter mass. The sizes of the disks were deduced to be of order 100 AU, comparable to the size of the clouds of material at the edge of the Solar System. The deductions from the IRAS data were confirmed in the case of β Pic by Smith and Terrile (1984) and others, who imaged the disk in the visible, scattered starlight (at 0.89 μm). Pantin *et al.* (1997) imaged the disk around β Pic at 12 μm and derived a radial density distribution out to 100 AU. Mauron and Dole (1999) attempted to detect the disk around Vega in polarized light at 0.44 μm. Most recently, the disks of the four prototypes have been imaged at 850 μm (Holland *et al.* 1998, Greaves *et al.* 1998), the disk of ϵ Eri being clearly resolved as a ring about the star. Other stars have been imaged in the near-infrared, namely HD98800 at 4.71 and 9.78 μm, showing there are two components in the near/mid infrared (Gehrz *et al.* 1999) and HD233517 (SAO26804) at 10 μm (Skinner *et al.* 1995).

A broad emission feature around 10 μm in the spectrum of β Pic was compared with the emission from Comets (Telesco and Knacke 1991, Knacke *et al.* 1993). Knacke *et al.* found that the emission from the dust around β Pic showed structure similar to that from the crystalline silicates found in some comets. Aitken *et al.* (1993) also found that the 10 μm silicate emission feature was similar to that in Comet Halley. Skinner *et al.* (1992) found silicate dust emission from HD98800. Sylvester *et al.* (1996) showed spectra around 10 μm for 13 Vega-like candidates, identifying silicate dust emission and features from carbon-rich molecules (UIRs) in some of them. Walker *et al.* (1996) and Butner *et al.* (1997) have also detected silicate emission from several Vega-like candidates around 10 μm. Butner *et al.* (2000) modeled their spectra using a model based on Comet Hale–Bopp data (which uses pyroxenes and olivines), obtaining good fits to the data for HD142666 and HD35187, but HD144432 required a pyroxene-to-olivine ratio higher than that for the other objects.

The original discovery of the four prototypes prompted several searches of the IRAS data for more main sequence stars with cool dust disks, and several lists of candidates have resulted, e.g., Walker and Wolstencroft (1988) (see also the review by Backman and Paresce 1993). The Infrared Space Observatory (ISO) was launched in November 1995 (Kessler *et al.* 1996) and was operational until April 1998 when the superfluid helium coolant finally ran out. The photometer on board ISO (ISOPHOT) operated between 2.5 and 240 μm, with a variety of detectors, filters, and observing modes (Lemke *et al.* 1996). Early results have shown the resolved dust disks around Vega (Heinrichsen *et al.* 1998) and β Pic (Heinrichsen *et al.* 1999) using high-resolution linear scans at 60 μm. Early maps show that several other disks can be resolved by ISO (Fajardo-Acosta *et al.* 1997, Walker *et al.* 1999) at 60 μm. The four prototype Vega-like stars were observed with ISOPHOT to investigate the properties of their dust disks in the infrared. Several candidate Vega-like stars were also observed, and the results for eight targets are given here.

II. OBSERVATIONS

Table I lists the targets observed. The spectral types came from the Bright Star Catalog or from Dunkin *et al.* (1997). Low-resolution spectra with the long wavelength channel, between 5.8 and 11.6 μm, were taken for all the objects (see Figs. 1 and 2). The long wavelength channel had a linear array of 64 pixels and a resolving power of $\sim$95. The aperture for the spectrometer was 24×24 arcsec, and the exposure time for the spectrum was 64 s. Small maps were made at 60 and 90 μm with the small camera on ISOPHOT, using the raster mode of the satellite, and additionally using the chopper in the ISOPHOT instrument to increase the sampling. The raster point step size was 60 arcsec and the line step size was 30 arcsec, with a chopper step of 15 arcsec. The camera had 9 pixels with a pixel size of 43.5×43.5 arcsec. HD144432 was not observed in the mapping mode, and the observation of HD142666 failed toward the end of the first map, at 60 μm, so no data were obtained at 90 μm. A high-resolution linear scan at 60 μm was made across the disk for four stars. The step size was 6 arcsec, which was matched to the point spread function and exploited the excellent pointing accuracy of the ISO satellite (see Heinrichsen *et al.* (1998) for more information). Calibration scans were made of γ Dra (HR6705), a star with no circumstellar material, to be used as a point source reference. Two scans were made for Vega, with a separation of around 325 days. The results from the two scans were identical, showing that the instrument remained stable during the mission. The two scans of Vega are shown in Fig. 3, the small offset in pointing on the first scan across Vega is not corrected, to show clearly the accuracy of the ISO pointing. HD142666 and HD169142 were observed once using the high-resolution scan mode. For β Pic, the disk was mapped using several high-resolution scans, at 25 and 60 μm (Heinrichsen *et al.* 1999).

The noise in the observation depends partly on the position in the ISO orbit, since the data taken soon after curing of the detectors (which happened twice per orbit) were less noisy and the responsivity of the detector could be more accurately determined. Observations taken near the beginning or end of the scientific window of the orbit had higher noise due to the Earth's radiation belts. The data were reduced from the raw data stage (ERD) using the ISOPHOT Interactive Analysis package, PIA 7.3, (Gabriel *et al.* 1997), which included a post-mission calibration update.

For the spectra, the dynamic spectral response correction (Klaas *et al.* 1997) was used, where each of the 64 pixels was calibrated using two calibration stars with similar fluxes at that

TABLE I
Spectrum Characteristics and Map Sizes for Targets Observed

Star	Sp. type	Spectrum	Map size 60/90 (″)	Angle (Z axis) (°)	Scan (60) (″)	Angle (°)	Tww (°)	T (°K)	Emissivity λ^n	Flux at 200 μm (Jy)	Dust mass ($M_\odot$)
Vega	A0V	Photosphere	24/36	112.2	19	103	95	65	−1.0	1.58	4.0×10^{-9}
β Pic	A5V	Cool thermal	26/28	43.1	12.4	30	105	65	−1.0	2.06	3.2×10^{-8}
Fomalhaut	A3V	Photosphere	19/30	59.0			80	55	−1.0	2.82	8.4×10^{-9}
ϵ Eri	K2V	Photosphere	—/—	71.8			90	50	−1.0	1.88	1.1×10^{-9}
49 Cet	A3V	Cool thermal	(7)/—	75.2			80	60	−1.0	0.32	5.5×10^{-8}
HD98800	K5Ve	Cool thermal	14/—	125.1			165	45:	−2.0	0.63	6.7×10^{-8}
HD139614	A7Ve	Silicate	—/—	109.6			135	45:	−1.5	3.92	4.5×10^{-6}
HD135344	F4Ve	Silicate	21/10	107.4			85	50	−1.1	9.53	8.1×10^{-5}
HD144432	A9/F0Ve	Silicate	xxxxx				180	50	−2.0	1.59	4.5×10^{-6}
HD169142	A5Ve	C-rich	—/54	84.7	(4.0)	90	115	55	−1.0	6.54	4.3×10^{-5}
HD34700	G0V	C-rich	12/—	58.3			100	60	−1.1	2.19	5.7×10^{-7}
HD142666	A8Ve	Silicate + C-rich	27/xx	101.6	7.8	102	175	110	0.0	2.58	6.7×10^{-6}

Note. The map size (the deconvolved full-width-half-maximum) is measured in the Z direction on the 60- and 90-μm maps. 49 Cet is not resolved at 60 μm. The angle is the position angle of the Z axis relative to North in the equatorial coordinate system. The scan (size) is the deconvolved Gaussian width at 60 μm from the high-resolution scan, where available. HD169142 is not resolved. The dust blackbody temperature and emissivity law are given, where they have been calculated from the ISOPHOT photometry between 60 and 240 μm. The blackbody temperature from Walker and Wolstencroft (1988) using IRAS data from 12 to 100 μm is given for comparison.

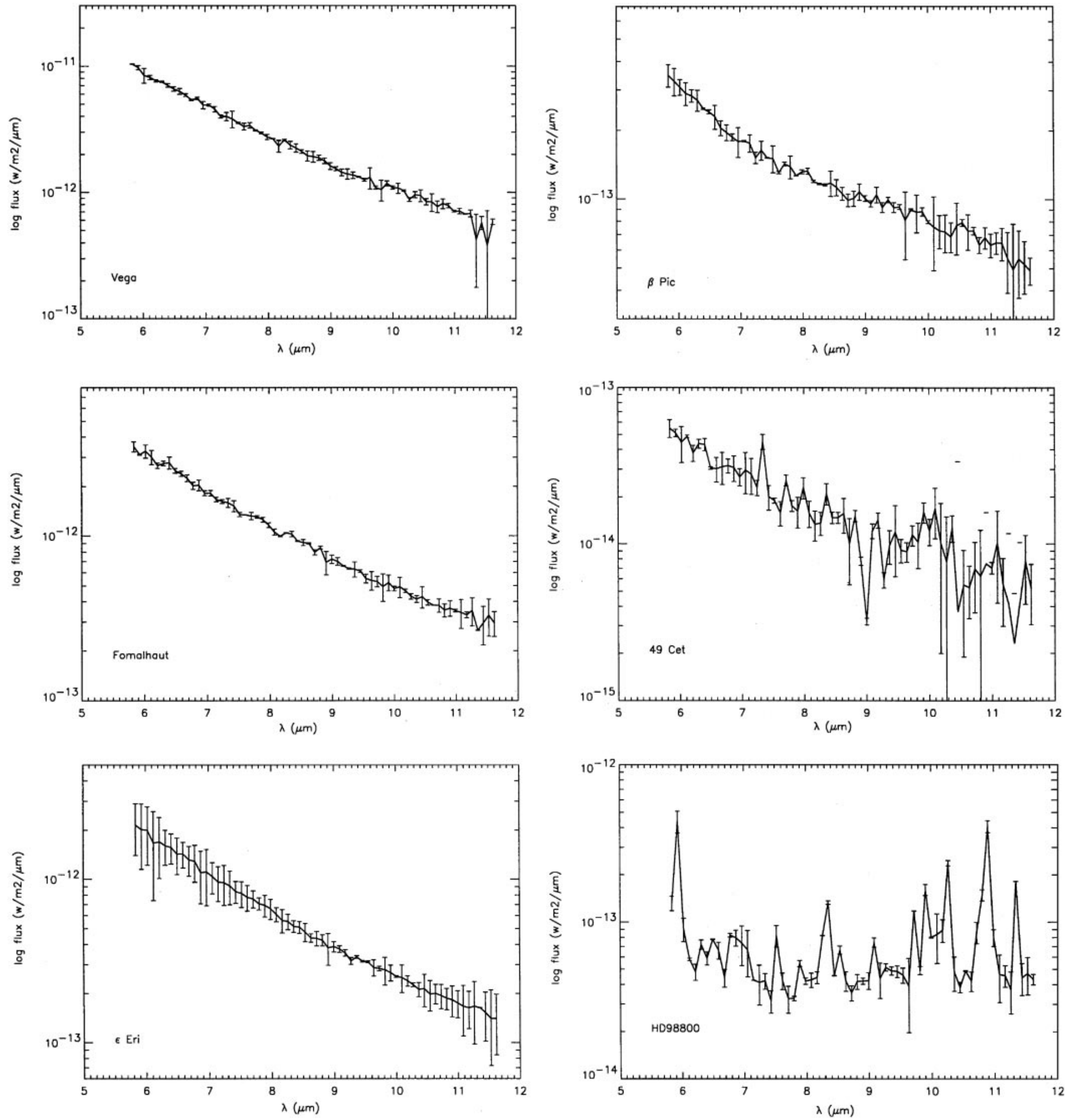

FIG. 1. Low-resolution spectra of Vega-like stars: the first column contains Vega, Fomalhaut, and ϵ Eri, and the second column contains β Pic, 49 Cet, and HD98800. The x axis is in micrometers, the y axis in watts per squared meter per micrometer.

wavelength. Vega was excluded from the calibration data set when the observed spectrum of Vega was processed. All stars with spectral types later than K1 were excluded from the calibration due to concern about a feature from SiO in their photospheres not included in the models. This meant that some pixels in some spectra had no close match to the observed flux, increasing the possible error in calibration (reflected as large error bars in Figs. 1 and 2). The absolute flux calibration is now better than 20%. The spectra of Fomalhaut and HD139614 were corrected for pointing errors, which were sufficiently large (+2.2

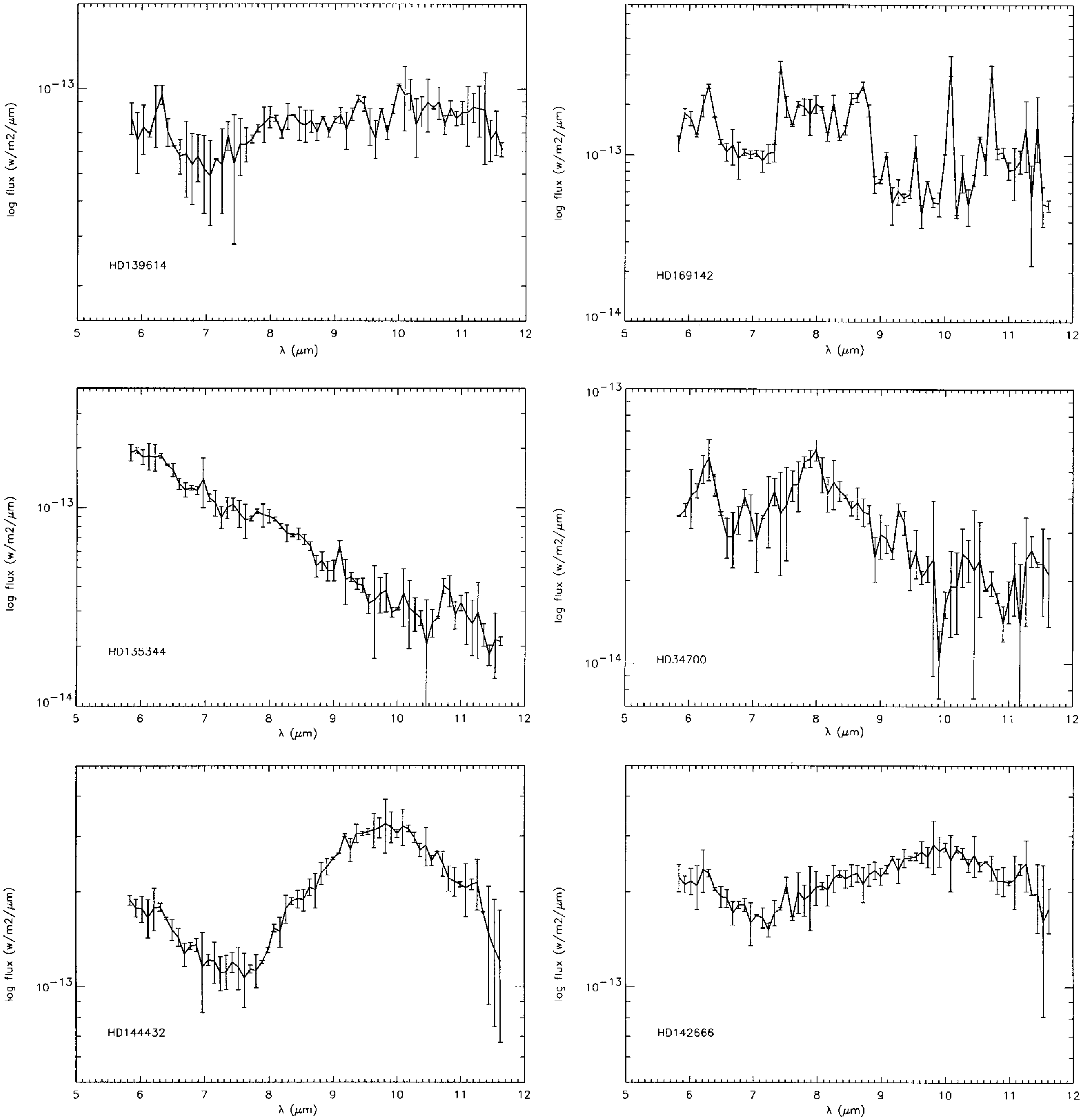

FIG. 2. Low-resolution spectra of Vega-like stars: the first column contains HD139614, HD135344, and HD144432, and the second column contains HD169142, HD34700, and HD142666. The *x* axis is in micrometers, the *y* axis in watts per squared meter per micrometer.

and −2.5 arcsec in spacecraft *Y* direction respectively) to affect the responsivity used.

For the maps and scans the internal calibration source (Schulz *et al.* 1999) was used to give the actual responsivity for that observation. However for the maps of HD169142, where the calibration source saturated the detector, and for the map of HD142666, where the observation failed before the second calibration observation, the orbital dependent default responsivity was used. For the maps, a calibration observation was taken at the start and at the end of the map in each filter, and the responsivity interpolated through the raster map. The data were deglitched at the second stage of processing and the first half of the data in

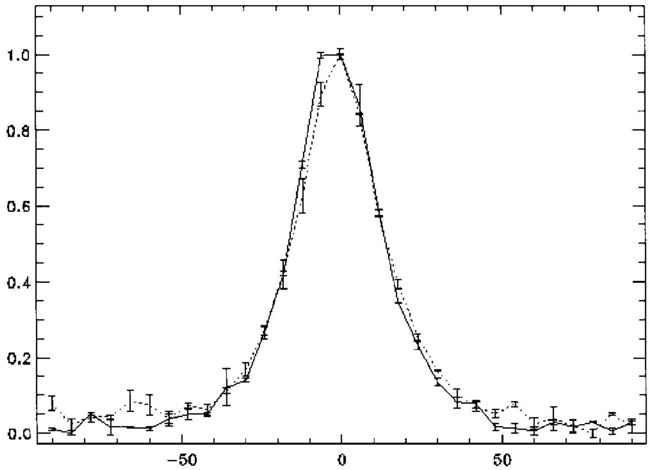

FIG. 3. Two high-resolution scans of Vega at 60 μm taken 325 days apart. The solid line shows the first scan, the dashed line the second scan. The flux is normalized to the peak value in each scan, and the x axis shows the offset (in arcseconds) from the center of the scan.

each chopper plateau was discarded to reduce the detector drift errors. The uncertainty in absolute flux level at 60 and 90 μm is 20%. For the photometry from 60 to 200 μm (at seven wavelengths—60, 80, 100, 120, 150, 170, and 200 μm) used to estimate the dust temperatures and emissivities, the uncertainty in absolute flux level is between 10 and 20%, dependent on the filter (see Klaas *et al.* 1998).

III. RESULTS

The spectra are shown in Fig. 1 and Fig. 2. The flux is given in watts per squared meter per micrometer and the uncertainty in the absolute flux level is 20%. The error bars shown in the figures are the formal uncertainty in the measurement, and do not include instrumental effects such as detector drift or pointing error, but do include the error from the dynamic spectral response correction. The spectra mainly confirm earlier work, but they do not have the large uncertainties around 9.7 μm due to the ozone correction from ground-based work, and they extend the spectra to 5.8 μm. For some objects (Vega, Fomalhaut, ϵ Eri) the stellar photosphere dominates the spectrum to 11.6 μm. The other spectra show either the cool thermal excess, the broad feature around 10 μm due to silicate dust emission, or the sharper molecular features due to carbon-rich molecules, often called UIRs (unidentified infrared features) or PAHs (polycyclic aromatic hydrocarbon molecules). The 6.2- and 7.7-μm features arise from C–C bonds, the 8.6- and 11.3-μm from C–H bonds.

The spectrum of β Pic shows excess emission from 8 μm onward, due to the thermal emission from the cool dust shell. The silicate emission feature is also present (see Butner *et al.* 2000), but the feature does not dominate this spectrum. The situation is similar for HD98800; however Sylvester *et al.* (1996) with their coverage to longer wavelengths show that HD98800 (SAO179815) has a very broad silicate dust emission feature. HD135344 and 49 Cet also show excess emission at the longer (spectral) wavelengths due to cool dust. HD169142 (Sylvester *et al.* show the 11.3-μm feature) and HD34700 show emission features at 6.2 and 7.7–8.6 μm from the C–C and C–H bonds, often attributed to PAHs. The 11.3-μm feature is not strong, but it occurs where the instrument sensitivity is lower. HD139614 may show a feature around 6.2 μm. The silicate feature for HD144432 is relatively sharp (see also Sylvester *et al.*), similar to that found from the dust around some young T Tau stars, such as GW Ori (Cohen and Witteborn 1985). HD142666 shows features from both silicate dust and carbon-rich molecules (particularly the 6.2- and the 11.3-μm features), the spectrum shown by Sylvester *et al.* (1996) may also show the 11.3-μm feature, noted by them as a point of inflection. The silicate dust can be attributed to olivines and pyroxenes, which may be similar to material found in primitive Solar System material (see Butner *et al.* 2000). Some comets, for example Comet Halley and Comet Bradfield 1987 XXIX, show the crystalline silicate feature at 11.2 μm, attributed to small olivine particles (Hanner *et al.* 1994).

The maps were orientated with respect to the spacecraft Z axis (see Fig. 4). The position angle of this axis in the astronomical equatorial coordinate reference frame (RA-Dec) is given in Table I. The width of the extended emission (in arcsec) at 60 and 90 μm around the star is only measured in the Z direction, because the detector response significantly affected the measurements along the scan lines in the Y direction (e.g., the "ghost" caused by the chopping can be seen in some of the maps in Fig. 4), and these effects have not been completely eliminated yet. For ease of comparison with other work, the sizes of the disks are expressed in terms of deconvolved full-width-half-maximum (FWHM) values in arcseconds; the FWHM is measured at 50% peak intensity, whereas the Gaussian width is measured at 60% of peak intensity. The width measured from the map is deconvolved using a width measured from a similar map of α Boo at 60 μm and γ Dra at 100 μm (scaled to 90 μm using the ISOPHOT Observer's manual) representing a point source, assuming the point spread function is Gaussian. The mapping mode of ISOPHOT is not scientifically validated due to the uncertainties in the detector drifts and the uncertainties in the value of the point spread function, so the numbers here must be treated with extreme caution (for example, the difference in values for HD142666 between the scan and the map).

The deconvolved Gaussian widths for the high-resolution scans, shown only for the 60-μm data, are given in Table I. The high-resolution linear scans made of β Pic and its accompanying comparison, γ Dra, showed the measurements are very close to the Gaussian function assumed (see Fig. 2 in Heinrichsen *et al.* 1999). The error in the measurement of the Gaussian width are estimated to be ± 2 arcsec. Although the observation of HD169142 gives a profile which is broader than the profile of γ Dra, the errors in the flux determination preclude any firm statement that the disk is resolved. Moriarty-Schieven *et al.* (2000) resolved the disk at 450 and 850 μm, and their results

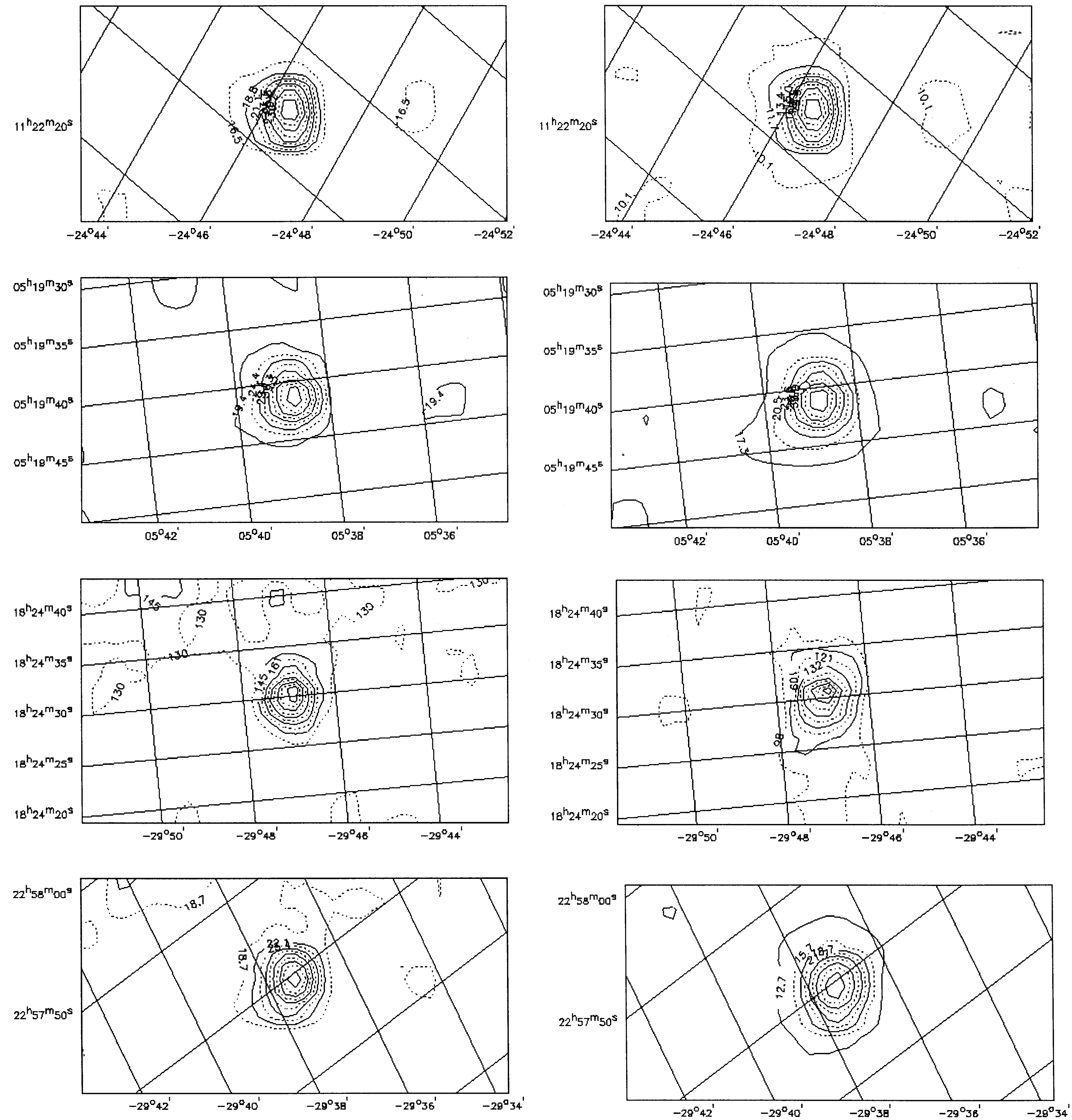

FIG. 4. Maps at 60 μm (left side) and 90 μm (right side) of four stars: HD98800 (top), HD34700, HD169142, and Fomalhaut (bottom). The flux densities are in megajansky per steradian and the maps are displayed in the spacecraft mapping orientation, with the RA-Dec grid overlaid. The spacecraft Y axis corresponds to the map x axis and the spacecraft Z axis corresponds to the map y axis. A "ghost" caused by the chopper throw can be seen on the right side of several maps.

showed that ISO did not scan the disk at the "best" angle. The disk around HD142666 is just resolved, and this represents the limit this technique could achieve. However, Moriarty-Schieven *et al.* (2000) did not resolve the disc at 450 or 850 μm, although the temperature derived for the dust (see Table I) is higher than that for the other targets.

A second high-resolution scan on Vega (Fig. 3) confirmed the results published earlier (Heinrichsen *et al.* 1998), showing the stability and reproducibility of the method. As the second scan was obtained at a different angle through the disk, it confirms that the Vega disk is symmetrical at the resolution obtainable with this method, although the scans did not cross the peak observed by Holland *et al.* (1998) at 850 μm.

IV. DISCUSSION

Photometry at seven wavelengths between 60 and 240 μm was taken, and the derived temperatures and emissivity laws are shown in Table I. The temperatures for Vega and β Pic, derived using this simple fit, are slightly different from the previously published values of 73 K with $\lambda^{-1.1}$ for Vega (Heinrichsen *et al.* 1998) and 85 K with λ^{-1} for β Pic (Heinrichsen *et al.* 1999), and hence reveal the uncertainties in this simple determination. The temperatures calculated here (see Table I) are lower than the blackbody temperatures derived by Walker and Wolstencroft (1988), which were calculated from up to four data points between 12 and 100 μm, showing that the longer wavelength coverage of ISO and the larger number of data points enabled the dust emissivity and the dust temperature to be determined. The dust temperature. The dust temperatures, emissivities, and 200-μm fluxes are used to estimate the dust mass (distances for the stars are given in Walker *et al.* (1999)), using the equation in Becklin and Zuckerman (1990). The values derived are in the range of 10^{-9} to 10^{-4} $M_\odot$, from less than the mass of the Moon to less than the mass of Jupiter.

The disk diameters for the four prototypes have been measured more precisely by Holland *et al.* (1998) and Greaves *et al.* (1998) at 850 μm (with a 15-m telescope as opposed to the 60-cm telescope in ISO), and they are able to measure the diameter of the inner edge of the dust disk. They get sizes of 24×21 arcsec for Vega, 22×11 arcses for β Pic, 41×18 arcsec for α PsA, and a peak ring width of 36 arcsec for ϵ Eri. The disks around Vega and β Pic have a characteristic diameter around 140 AU, calculated from the Gaussian widths of the high-resolution scans. HD142666 is much further away than Vega and β Pic, with a distance of possibly almost 300 pc (Walker and Wolstencroft 1988), which means that the diameter of the dust disk must be around 1000 AU, comparable to disks around young stars. (HD142666 is not in the Hipparcos catalogue, but the parallax uncertainties of stars in the area suggest a lower limit to the distance of around 300 pc.) The sizes (in arcseconds) from the maps, at this stage of our understanding of the ISOPHOT detector behavior, should be taken more as an indicator as to whether the disk is "resolved" or "not resolved" depending on whether the width is significantly larger than the value used for the point spread function (58.7 arcsec at 60 μm, from α Boo, and 64.8 arcsec at 90 μm from the scaled γ Dra observation at 100 μm). The disks around ϵ Eri, 49 Cet, and HD139614 are not resolved at either wavelength. The ring around ϵ Eri is face-on and ISO is more sensitive to warm dust, so the dust observed with ISO may well be from regions inside the ring detected at 850 μm, and hence not resolved. The Vega-like candidates studied here are probably younger than the Sun, since they have residual emission features in their absorption lines (Dunkin *et al.* 1997), and the disks contain more material than Vega and β Pic (allowing them to be studied at their greater distances), so these stars may represent a precursor phase when material is starting to form into larger bodies, and planet formation will soon commence.

ACKNOWLEDGMENTS

This paper has been based on observations with ISO, an ESA mission with instruments funded by ESA member states (especially the PI countries: France, Germany, the Netherlands and the United Kingdom) and with the participation of ISAS and NASA. The data in this paper were reduced with PIA, a joint development by the ESA Astrophysics Division and the ISOPHOT Consortium led by the Max Planck Institute for Astronomy (MPIA). Our thanks go to colleagues at MPIA (U. Klaas, P. Ábrahám, M. Haas) and Rutherford Appleton Laboratory (RAL) (P. Richards and H. Morris) for their help with the data reduction.

REFERENCES

Aitken, D. K., T. J. T. Moore, P. F. Roche, C. H. Smith, and C. M. Wright 1993. Mid-infrared spectroscopy of Beta Pictoris: Constraints on the dust grain size. *Mon. Not. R. Astron. Soc.* **265**, L41–L43.

Aumann, H. H., F. C. Gillett, C. A. Beichman, T. de Jong, J. R. Houck, F. J. Low, G. Neugebauer, R. G. Walker, and P. R. Wesselius 1984. Discovery of a shell around Alphae Lyrae. *Astrophys. J.* **278**, L23–L28.

Backman, D. E., and F. Paresce 1993. Main-sequence stars with circumstellar solid material: The Vega phenomenon. In *Protostars and Planets III* (E. H. Levy and J. I. Lunine, Eds.), pp. 1253–1304. Univ. of Arizona Press, Tuscon.

Becklin, E. E., and B. Zuckerman 1990. Submillimeter emission from small dust grains orbiting nearby stars. In *Submillimetre Astronomy* (G. D. Watt and A. S. Webster, Eds.), pp. 147–153. Kluwer, Dordrecht.

Butner, H. M., H. J. Walker, D. H. Wooden, and F. C. Witteborn 1997. Examples of comet-like spectra among β Pic-like stars. In *Astronomical and Biochemical Origins and the Search for Life in the Universe*. (C. B. Cosmovici, S. Bowyer, and D. Wertheimer, Eds.), pp. 149–155. Editrice Compositori, Bologna.

Butner, H. M., H. J. Walker, D. H. Wooden, and F. C. Witteborn 2000. The comet-like mid-infrared spectra of Vega-like stars. *Icarus*, submitted.

Cohen, M., and F. C. Witteborn 1985. Spectrophotometry at 10 microns of T Tauri stars. *Astrophys. J.* **294**, 345–356.

Dunkin, S. K., M. J. Barlow, and S. G. Ryan 1997. High-resolution spectroscopy of Vega-like stars—I. Effective temperatures, gravities and photospheric abundances. *Mon. Not. R. Astron. Soc.* **286**, 604–616.

Fajardo-Acosta, S. B., R. E. Stencel, and D. E. Backman 1997. Infrared Space Observatory mapping of 60 micron dust emission around Vega-type systems. *Astrophys. J.* **487**, L151–L154.

Gabriel, C., J. Acosta-Pulido, I. Heinrichsen, H. Morris, and W.-M. Tai 1997. The ISOPHOT Interactive Analysis PIA, a calibration and scientific analysis tool. In *Astronomical Data Analysis Software and Systems VI* (G. Hunt and H. E. Payne, Eds.), *Astron. Soc. Pac. Conf. Ser.*, Vol. 125, pp. 108–112.

Gehrz, R. D., N. Smith, F. J. Low, J. Krautter, J. G. Nollenberg, and T. J. Jones 1999. Thermal infrared images of the remarkable young nearby multiple star HD 98800. *Astrophys. J.* **512**, L55–L58.

Gillett, F. C. 1986. IRAS observations of cool excess around main sequence stars. In *Light on Dark Matter* (F. P. Israel, Ed.), pp. 61–69. Reidel, Dordrecht.

Greaves, J. S., W. S. Holland, G. Moriarty-Schieven, T. Jenness, W. R. F. Dent, B. Zuckerman, C. McCarthy, R. A. Webb, H. M. Butner, W. K. Gear, and

H. J. Walker 1998. A dust ring around Epsilon Eridani: Analogue to the young Solar System. *Astrophys. J.* **506**, L133–L137.

Hanner, M. S., D. K. Lynch, and R. W. Russell 1994. The 8–13 micron spectra of comets and the composition of silicate grains. *Astrophys. J.* **425**, 274–285.

Heinrichsen, I., H. J. Walker, and U. Klaas 1998. Infrared mapping of the dust disc around Vega. *Mon. Not. R. Astron. Soc.* **293**, L78–L82.

Heinrichsen, I., H. J. Walker, U. Klaas, R. J. Sylvester, and D. Lemke 1999. An infrared image of the dust disc around β Pic. *Mon. Not. R. Astron. Soc.* **304**, 589–594.

Holland, W. S., J. S. Greaves, B. Zuckerman, R. A. Webb, C. McCarthy, I. M. Coulson, D. M. Walther, W. R. F. Dent, W. Gear, and I. Robson 1998. Submillimetre images of dusty debris around nearby stars. *Nature* **392**, 788–791.

Kessler, M. F., J. A. Steinz, M. E. Anderegg, J. Clavel, G. Drechsel, P. Estaria, J. Faelker, J. R. Riedinger, A. Robson, B. G. Taylor, and S. Ximénez de Ferrán 1996. The Infrared Space Observatory (ISO) mission. *Astron. Astrophys.* **315**, L27–L31.

Klaas, U., and 11 colleagues 1997. ISOPHOT-S: Capabilities and calibration. In *First ISO Workshop on Analytical Spectroscopy*. (A. M. Herus, K. Leech, N. R. Trams, M. Perry, Eds.), ESA SP-419, pp. 113–116. ESA Publications Divison, Noordwijk.

Klaas, U., R. J. Laureijs, M. Radovich, and B. Schulz 1998. ISOPHOT calibration accuracies. ESA SAI/98-092/Dc Version 2.

Knacke, R. F., S. B. Fajardo-Acosta, C. M. Telesco, J. A. Hackwell, D. K. Lynch, and R. W. Russell 1993. The silicates in the disk of β Pictoris. *Astrophys. J.* **418**, 440–450.

Lemke, D., and 49 colleagues 1996. ISOPHOT—Capabilities and performance. *Astron. Astrophys.* **315**, L64–L70.

Mauron, N., and H. Dole 1999. An attempt to detect the dust disk of Vega by photopolarimetry, and constraints on the grain size. *Astron. Astrophys.* **337**, 803–814.

Moriarty-Schieven, G. H., H. M. Butner, and H. J. Walker 2000. Extended dust emission from Vega-like stars. *Icarus*, submitted.

Pantin, E., P. O. Lagage, and P. Artymowicz 1997. Mid-infrared images and models of the β Pictoris dust disk. *Astron. Astrophys.* **327**, 1123–1136.

Schulz, B., and 13 colleagues 1999. ISOPHOT photometric calibration of point sources. In *The Universe as Seen by ISO* (P. Cox and M. F. Kessler, Eds.), SP-427, pp. 89–92. ESA Publications Divison, Noordwijk.

Skinner, C. J., M. J. Barlow, and K. Justtanont 1992. Silicate dust in a Vega-excess system. *Mon. Not. R. Astron. Soc.* **255**, 31–36.

Skinner, C. J., R. J. Sylvester, J. R. Graham, M. J. Barlow, M. Meixner, E. Keto, J. F. Arens, and J. G. Jernigan 1995. The dust disk around the Vega-excess star SAO26804. *Astrophys. J.* **444**, 861–873.

Smith, B. A., and R. T. Terrile 1984. A circumstellar disk around β Pictoris. *Science* **226**, 1421.

Sylvester, R. J., C. J. Skinner, M. J. Barlow, and V. Mannings 1996. Optical, infrared and millimetre-wave properties of Vega-like systems. *Mon. Not. R. Astron. Soc.* **279**, 915–939.

Telesco, C. M., and R. F. Knacke 1991. Detection of silicates in the β Pictoris disk. *Astrophys. J.* **372**, L29–L31.

Walker, H. J., and R. D. Wolstencroft 1988. Cool circumstellar matter around nearby main sequence stars. *Publ. Astron. Soc. Pacific* **100**, 1509–1521.

Walker, H. J., H. M. Butner, D. Wooden, and F. Witteborn 1996. Silicate dust around β-Pic-like stars. In *The Role of Dust in the Formation of Stars* (H. U. Käufl and R. Siebenmorgen, Eds.), pp. 223–226. Springer-Verlag, Berlin/Heidelberg.

Walker, H. J., I. Heinrichsen, U. Klaas, and R. J. Sylvester 1999. Infrared mapping of the dust around main sequence stars. In *The Universe as Seen by ISO* (P. Cox and M. F. Kessler, Eds.), SP-427, pp. 425–428. ESA Publications Divison, Noordwijk.